

Acknowledgements

We thank R. Colella and J. Wark for discussions, and D. Arms for technical support. This work was conducted at the MHATT-CAT insertion device beamline at the Advanced Photon Source. Use of the Advanced Photon Source was supported by the US Department of Energy Basic Energy Sciences, Office of Energy Research. We also acknowledge partial support from the National Science Foundation, the Center for Ultrafast Optical Science, and the AFOSR through the MURI programme.

Correspondence and requests for materials should be addressed to M.E.D. (e-mail: mattydee@umich.edu).

Spin-dependent exciton formation in  $\pi$ -conjugated compounds

J. S. Wilson\*, A. S. Dhoot\*, A. J. A. B. Seeley\*, M. S. Khan†, A. Köhler\* & R. H. Friend\*

\* Cavendish Laboratory, Madingley Road, Cambridge, CB3 0HE, UK  
 † Department of Chemistry, Sultan Qaboos University, Al-Khod 123, Oman

The efficiency of light-emitting diodes (LEDs) made from organic semiconductors is determined by the fraction of injected electrons and holes that recombine to form emissive spin-singlet states rather than non-emissive spin-triplet states. If the process by which these states form is spin-independent, the maximum efficiency of organic LEDs will be limited to 25 per cent<sup>1</sup>. But recent reports have indicated fractions of emissive singlet states ranging from 22 to 63 per cent<sup>2–5</sup>, and the reason for this variation remains unclear. Here we determine the absolute fraction of singlet states generated in a platinum-containing conjugated polymer and its corresponding monomer. The spin-orbit coupling introduced by the platinum atom allows triplet-state emission, so optically and electrically generated luminescence from both singlet and triplet states can be compared directly. We find an average singlet generation fraction of  $22 \pm 1$  per cent for the monomer, but  $57 \pm 4$  per cent for the polymer. This suggests that recombination is spin-independent for the monomer, but that a spin-dependent process, favouring singlet formation, is effective in the polymer. We suggest that this process is a consequence of the exchange interaction, which will operate on overlapping electron and hole wavefunctions on the same polymer chain at their capture radius.

Several sophisticated methods have been used to determine the singlet generation fraction in organic LEDs, but these are often complicated by the fact that triplet states are generally non-emissive in conjugated organic compounds. As a result it has previously only been possible to place a lower limit on the singlet generation fraction in polymer LEDs. We have circumvented the problem of a non-emissive triplet state by investigating a Pt-containing polymer and its corresponding monomer (Fig. 1). The heavy Pt atom introduces spin-orbit coupling which allows the spin of the electron to flip or rephase and transitions between the singlet and triplet manifolds become possible<sup>6</sup>. Conjugation is preserved through the Pt atom by mixing of the frontier orbitals of the Pt and the ligand<sup>7</sup>. Direct emission from the triplet state is therefore observed for both optical and electrical excitation of LEDs made from these materials and this allows a straightforward calculation of the absolute singlet generation fraction.

The photoluminescence and electroluminescence spectra of the polymer and monomer (Fig. 2) both show two characteristic emission bands, and the relative contribution of each band to the total emission is indicated as a percentage. The high and low energy bands are due to singlet and triplet excited states  $S_1$  and  $T_1$ ,

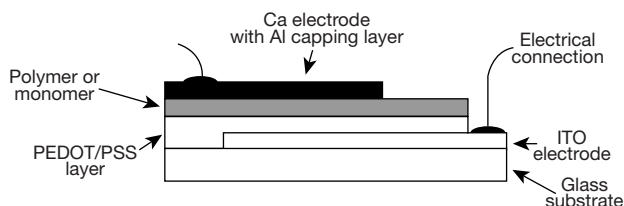
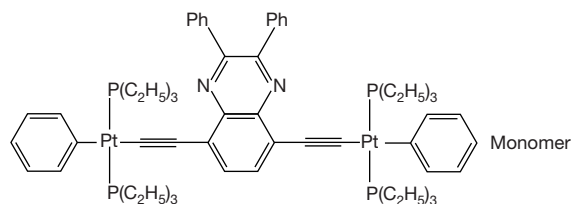
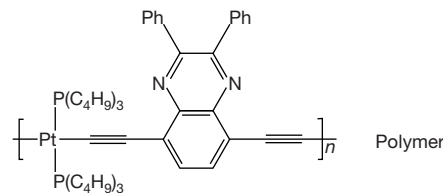


Figure 1 The chemical structures of the platinum-containing polymer and monomer investigated. A schematic of the simple light-emitting diode structure used is also given. PEDOT, poly(3,4-ethylenedioxythiophene); PSS, poly(styrenesulphonate); ITO, indium-tin oxide.

respectively. The triplet-state emission of this polymer and monomer and that of other similar materials has been well characterized previously by lifetime and photoinduced absorption measurements<sup>8–11</sup>. The triplet emission is observed at around 0.7 eV below the singlet in this and other conjugated polymers<sup>9,10,12–14</sup> and this finite exchange energy implies an excited state which is self-localized.

We note that although the spin-orbit coupling induced by the heavy Pt atom has been shown to produce close to 100% intersystem crossing<sup>8</sup> from the  $S_1$  state to  $T_1$ , there is still more emission observed from  $S_1$  than from  $T_1$  in photoluminescence at 290 K. This is because, despite the  $T_1-S_0$  transition being partially allowed in this polymer and monomer, the radiative decay rates from the triplet states are still only of the order of  $10^3 \text{ s}^{-1}$  in comparison with non-radiative decay rates of  $10^6-10^5 \text{ s}^{-1}$ , so only one in 1,000 of the triplets generated emits<sup>15</sup>. The non-radiative decay rate increases exponentially with decreasing  $T_1-S_0$  gap and is controlled by multi-phonon emission<sup>15</sup>.

In order to compare electroluminescence and photoluminescence spectra we measured both in LED structures. For electrical excitation we observe a greater percentage of the photons to be from the triplet state than with optical excitation, but in other respects the spectra are very similar (Fig. 2). In order to use the emission spectra to calculate the fraction of excited states generated in the singlet spin state,  $\chi_S$ , we model the processes of photoluminescence and electroluminescence as shown in Fig. 3. In photoluminescence a number  $I$  of excitons are originally all created in the singlet  $S_1$  state, and from there they decay radiatively (with a decay rate  $k_{R(S)}$ ) or non-radiatively (with a decay rate  $k_{NR(S)}$ ) to the singlet ground state  $S_0$ , or undergo intersystem crossing to the triplet manifold (with a rate  $k_{ISC}$ ). Both radiative and non-radiative decay occurs from the triplet state  $T_1$  to the ground state  $S_0$ . For electroluminescence the processes are exactly the same as in photoluminescence, with the important exception that it is also possible to create a fraction  $\chi_T$  of triplet excitons directly. We define the quantum yields

$\Phi$  for radiative triplet (TR) and singlet (SR) emission and for intersystem crossing (ISC):

$$\Phi_{SR} = \frac{k_{R(S)}}{[k_{ISC} + k_{R(S)} + k_{NR(S)}]} \quad \Phi_{TR} = \frac{k_{R(T)}}{[k_{R(T)} + k_{NR(T)}]}$$

$$\Phi_{ISC} = \frac{k_{ISC}}{[k_{ISC} + k_{R(S)} + k_{NR(S)}]}$$

The number of photons emitted from the triplet and singlet states are denoted  $N_T$  and  $N_S$  respectively, and the ratio of these is labelled  $R$ . For photoluminescence:

$$N_{S,PL} = I\Phi_{SR,PL}$$

$$N_{T,PL} = I\Phi_{ISC,PL}\Phi_{TR,PL}$$

$$R_{PL} = \frac{N_{T,PL}}{N_{S,PL}} = \frac{\Phi_{ISC,PL}\Phi_{TR,PL}}{\Phi_{SR,PL}}$$

For electroluminescence:

$$N_{S,EL} = I\chi_S\Phi_{SR,EL}$$

$$N_{T,EL} = I\chi_S\Phi_{ISC,EL}\Phi_{TR,EL} + I\chi_T\Phi_{TR,EL}$$

$$R_{EL} = \frac{N_{T,EL}}{N_{S,EL}} = \frac{\chi_S\Phi_{ISC,EL}\Phi_{TR,EL} + \chi_T\Phi_{TR,EL}}{\chi_S\Phi_{SR,EL}}$$

Comparing photoluminescence and electroluminescence gives:

$$\frac{R_{PL}}{R_{EL}} = \left( \frac{\chi_S\Phi_{ISC,PL}}{\chi_S\Phi_{ISC,EL} + \chi_T} \right) \left( \frac{\Phi_{TR,PL}}{\Phi_{TR,EL}} \right) \left( \frac{\Phi_{SR,EL}}{\Phi_{SR,PL}} \right) \quad (1)$$

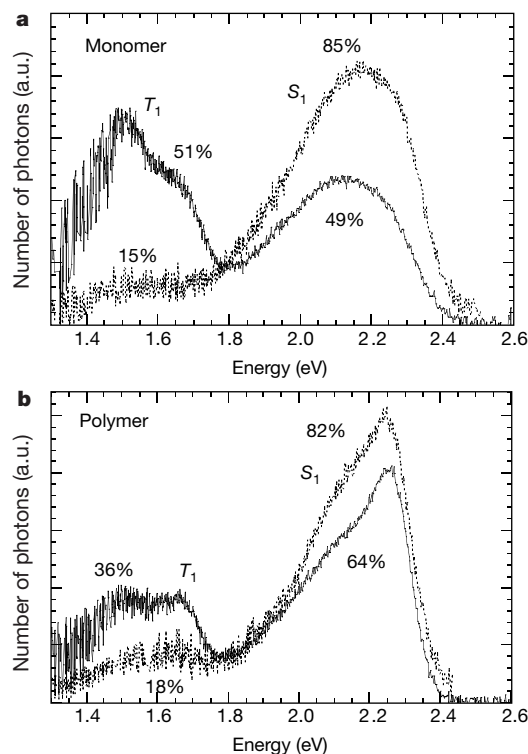


**Figure 2** Comparison of the photoluminescence and electroluminescence spectra of light-emitting diodes of the platinum-containing polymer and monomer at 290 K. **a**, The photoluminescence (dotted line) and electroluminescence (solid line) spectra of a monomer LED. **b**, The photoluminescence and electroluminescence spectra of a polymer LED. The triplet emission is denoted by  $T_1$  and the singlet emission by  $S_1$ . The spectra have been plotted in terms of number of photons and the fraction of the total emission that the singlet and triplet emission represent are given as percentages.

If we assume that the decay rates are the same for electroluminescence and photoluminescence we obtain  $\Phi_{PL} = \Phi_{EL}$ , and because  $\chi_S + \chi_T = 1$ , equation (1) becomes:

$$\frac{R_{PL}}{R_{EL}} = \left( \frac{\chi_S\Phi_{ISC,PL}}{\chi_S\Phi_{ISC,EL} + (1 - \chi_S)} \right) \quad (2)$$

For these materials  $\Phi_{ISC}$  is known to be close to one<sup>8</sup> so we approximate equation (2) by:

$$\frac{R_{PL}}{R_{EL}} = \chi_S \quad (3)$$

Therefore, simply by dividing the spectrally integrated triplet emission by that of singlet emission for electroluminescence and photoluminescence in spectra such as those in Fig. 2, it is possible to obtain an absolute value for the singlet generation fraction,  $\chi_S$ , with the advantage that many factors involved cancel out. For example for the data shown in Fig. 2b,  $R_{PL} = 18/82$ , and  $R_{EL} = 36/64$  which gives  $\chi_S = 0.39$ .

The only assumption that has been made is that there is no difference in the decay rates for excited states whether they are created optically or electrically and we now examine this more closely. If electroluminescence and photoluminescence originate from different positions in the device relative to the electrodes, they may experience different quenching<sup>16,17</sup>. To check this we measured the dependency of  $\chi_S$  on film thickness (Fig. 4a) and also the lifetimes (and therefore decay rates<sup>6</sup>) of triplet emission for both optical and electrical excitation. We find no significant variations in  $\chi_S$  down to devices where the emitting layer was only around 20 nm thick and we observe the same lifetimes in photoluminescence and electroluminescence. For the monomer the room-temperature triplet lifetime is  $10 \pm 2 \mu\text{s}$  for optical excitation and  $11.8 \pm 0.5 \mu\text{s}$  for electrical excitation. For the polymer the room temperature lifetime is shorter and therefore more difficult to measure, but at around 100 K optical excitation gives a triplet lifetime of  $2.8 \pm 0.8 \mu\text{s}$  and electrical excitation gives  $3 \pm 1 \mu\text{s}$ . The decay rates of the triplet are therefore the same for both optical and electrical excitation.

In order to elucidate which parameters control the generation of singlet and triplet excited states in organic LEDs we studied the dependence of the singlet generation fraction on electric field and temperature. The temperature may affect carrier mobilities and processes with an activation energy, and the electric field could also influence exciton formation<sup>18</sup>. However, it can be seen from Fig. 4b and c that we observe no significant variation in  $\chi_S$  with temperature or electric field over the working range of the devices. We note that the room-temperature values for  $\chi_S$  are slightly lower than the values below 200 K, but we cannot rule out a systematic error here as

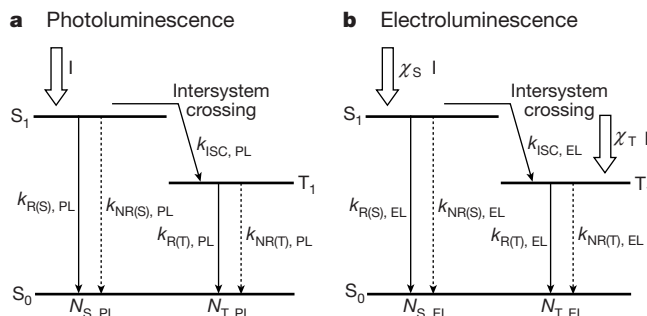


**Figure 3** A simple model for the emission spectra in photoluminescence (**a**) and electroluminescence (**b**).  $I$  represents an initial number of excitons.  $k_{NR}$ ,  $k_R$  and  $k_{ISC}$  represent non-radiative, radiative and intersystem crossing rates respectively, and  $N_S$  and  $N_T$  represent the number of singlet and triplet photons that would be expected to be emitted.  $\chi_S$  and  $\chi_T$  are the singlet and triplet generation fractions, respectively.  $S_0$  is the singlet ground state.

there is very little triplet emission in photoluminescence at 290 K.

To summarize, we find different values of the singlet generation fraction  $\chi_S$  for the polymer and monomer of the same material that reconcile the different values available in the literature. The average values of  $\chi_S$  we obtain for the monomer and polymer at room temperature are  $0.15 \pm 0.01$  and  $0.40 \pm 0.03$  respectively, and averaging over all temperatures gives  $0.22 \pm 0.01$  and  $0.57 \pm 0.04$  respectively. For the monomer this is close to the 0.25 expected from simple spin statistics and in agreement with the value of  $0.22 \pm 0.03$  measured<sup>2</sup> for the small molecule Alq<sub>3</sub>. For the polymer the average value of  $\chi_S$  is more than double the value expected from simple spin statistics and is above the lower limit for the singlet generation fraction of 0.35–0.5 measured for PPV derivative polymers<sup>3,4</sup>. The 290 K value also agrees with the  $\chi_S$  value of 0.4 predicted<sup>5</sup> for a polymer with a bandgap between 2.3 and 2.5 eV. Clearly the fact that we observe  $\chi_S$  to be largely independent of temperature and applied electric field means these parameters do not significantly influence the probability of forming either a singlet or triplet spin state.

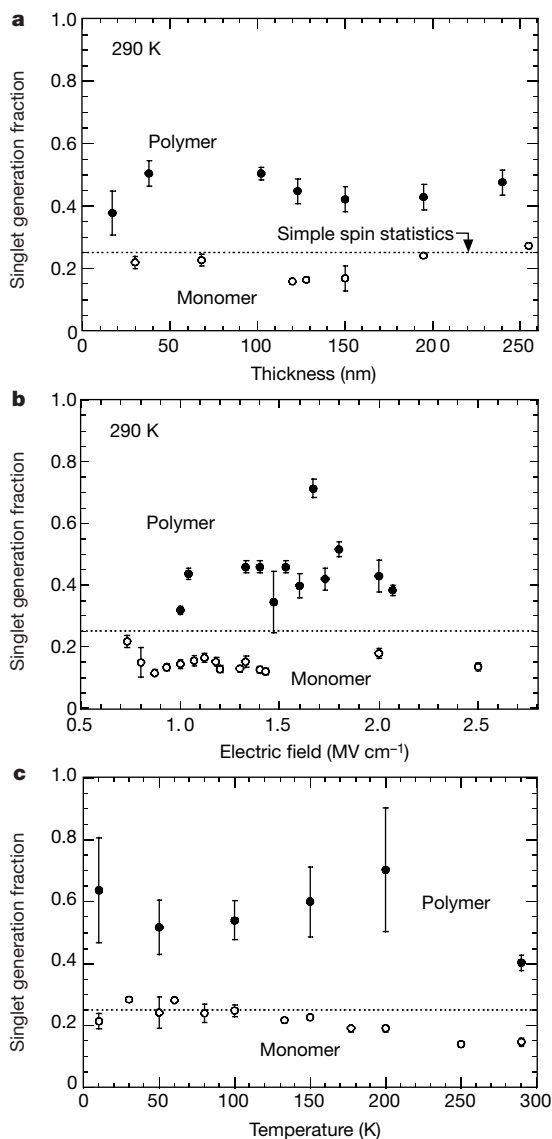


**Figure 4** The singlet generation fraction  $\chi_S$  for the platinum-containing polymer and monomer under different device conditions. **a**,  $\chi_S$  plotted as a function of device thickness for polymer (solid circles) and monomer (open circles) LEDs. **b**,  $\chi_S$  plotted as a function of applied electric field. **c**,  $\chi_S$  plotted as a function of temperature. The error bars on each point represent the statistical error obtained by measuring a large number of devices. The dotted line represents the fraction (0.25) expected from simple spin statistics.

The marked difference we find in  $\chi_S$  for polymer and monomer LEDs implies different processes of singlet and triplet formation via electron–hole capture and we now consider why these may occur. Organic LEDs operate by injection of electrons and holes from opposite electrodes, and transport by hopping from one molecular site (or polymer chain) to another. Electron and hole capture one another when they are held within their mutually attractive potential, and this process is usually described using the Langevin model<sup>19,20</sup>. Typical capture radii are about 10 nm. The distinction between molecular semiconductors and conjugated polymers is that this distance is considerably greater than a molecular dimension, but comparable to the delocalization lengths for electron and hole wavefunctions on polymer chains. Therefore, for molecular materials, electron–hole capture is achieved at a range where only the Coulomb interaction is effective, and the process is independent of the final spin state of the exciton (even though the rates for the final step of exciton formation may be spin-dependent). In contrast, for the polymers, when electron and hole are present on the same chain at the capture range, the interaction between them results also from direct overlap of electron and hole wavefunctions, and is therefore spin-dependent (through the exchange interaction). Thus, the probability of electron–hole capture is now spin-dependent. Our results demonstrate that singlets are favoured over triplets, and there are a number of processes which might be responsible for this<sup>5,18,21–23</sup>. These include the greater spatial extension along the polymer chain of the singlet exciton, giving a stronger longer-range attraction<sup>14</sup>; or the closer energy match between the electron–hole and the singlet exciton compared to the triplet exciton<sup>18</sup>. Spin-dependent interactions at this point of electron–hole capture give spin-dependent singlet–triplet generation fractions because the probability of forming the exciton over electron and hole moving apart is spin-dependent.

Thus, direct observation of triplet emission has allowed us to demonstrate that there is a different quantum-mechanical process of electron–hole capture in operation in organic compounds with an extended conjugated system as compared to small conjugated molecules. In particular, the process of electron–hole capture in conjugated polymers is dependent on the final spin state. The high singlet generation fractions found in conjugated polymers<sup>3–5</sup> suggest that it may not be necessary to harvest triplets in these materials in order to create efficient LEDs. □

**Methods**

Single-layer light-emitting diodes of the platinum-containing polymer and monomer were fabricated according to the structure shown in Fig. 1 by spin-coating and subsequent thermal evaporation of the metal electrodes. Measurements of photoluminescence and electroluminescence were made with the LEDs in a continuous-flow helium cryostat. For photoluminescence, excitation was provided by the 457-nm line of a continuous wave argon ion laser, incident almost perpendicular to the indium-tin oxide (ITO) side of the devices. Measurements of electroluminescence spectra were made with the devices in exactly the same configuration as for photoluminescence and with a constant voltage supplied by a Keithley 230 voltage source. The photoluminescence and electroluminescence emission spectra were recorded perpendicular to the devices by using a spectrograph with an optical fibre input coupled to a cooled charge-coupled device (CCD) array (Oriel Instaspec IV). For the photoluminescence lifetime measurements, the tripled output from a Q-switched YAG laser was used (355 nm, ~15 ns pulses). For the electroluminescence lifetime measurements, square wave electrical pulses (15–30 V, 500  $\mu$ s pulses) were applied to the devices. In both cases the transient emission was recorded by using a photomultiplier tube and a digital oscilloscope. Lifetimes were calculated by fitting the decay curves to an exponential. All measurements were made under vacuum or in a He atmosphere of 10 mbar.

Received 5 July; accepted 28 August 2001.

1. Friend, R. H. *et al.* Electroluminescence in conjugated polymers. *Nature* **397**, 121–128 (1999).
2. Baldo, M. A., O'Brien, D. F., Thompson, M. E. & Forrest, S. R. Excitonic singlet–triplet ratio in a semiconducting organic thin film. *Phys. Rev. B* **60**, 14422–14428 (1999).
3. Ho, P. K. H. *et al.* Molecular-scale interface engineering for polymer light-emitting diodes. *Nature* **404**, 481–484 (2000).
4. Cao, Y., Parker, I. D., Yu, G., Zhang, C. & Heeger, A. J. Improved quantum efficiency for electroluminescence in semiconducting polymers. *Nature* **397**, 414–417 (1999).
5. Wohlgenannt, M., Tandon, K., Mazumdar, S., Ramasesha, S. & Vardeny, Z. V. Formation cross-sections of singlet and triplet excitons in  $\pi$ -conjugated polymers. *Nature* **409**, 494–497 (2001).

6. Turro, N. J. *Modern Molecular Photochemistry* 1–195 (University Science, California, 1991).
7. Beljonne, D. *et al.* Spatial extent of the singlet and triplet excitons in transition metal-containing polyynes. *J. Chem. Phys.* **105**, 3868–3877 (1996).
8. Wittmann, H. F., Friend, R. H., Khan, M. S. & Lewis, J. Optical spectroscopy of platinum and palladium containing polyynes. *J. Chem. Phys.* **101**, 2693–2698 (1994).
9. Wilson, J. S. *et al.* Triplet states in a series of Pt-containing ethynyls. *J. Chem. Phys.* **113**, 7627–7634 (2000).
10. Chawdhury, N. *et al.* Evolution of lowest singlet and triplet excited states with number of thienyl rings in platinum polyynes. *J. Chem. Phys.* **110**, 4963–4970 (1999).
11. Chawdhury, N. *et al.* Synthesis and electronic structure of platinum-containing polyynes with aromatic and heteroaromatic rings. *Macromolecules* **31**, 722–727 (1998).
12. Romanovskii, Y. V. *et al.* Phosphorescence of  $\pi$ -conjugated oligomers and polymers. *Phys. Rev. Lett.* **84**, 1027–1030 (2000).
13. Hertel, D. *et al.* Phosphorescence in conjugated poly(para-phenylene)-derivatives. *Adv. Mater.* **13**, 65–70 (2001).
14. Beljonne, D., Shuai, Z., Friend, R. H. & Brédas, J. L. Theoretical investigation of the lowest singlet and triplet states in poly(paraphenylene vinylene) oligomers. *J. Chem. Phys.* **102**, 2042–2049 (1995).
15. Wilson, J. S. *et al.* The energy gap law for triplet states in Pt-containing conjugated polymers and monomers. *J. Am. Chem. Soc.* **123**, 9412–9417 (2001).
16. Becker, H., Burns, S. E. & Friend, R. H. Effect of metal films on the photoluminescence and electroluminescence of conjugated polymers. *Phys. Rev. B* **56**, 1893–1905 (1997).
17. Kim, J. S., Ho, P. K. H., Greenham, N. C. & Friend, R. H. Electroluminescence emission pattern of organic light-emitting diodes: Implications for device efficiency calculations. *J. Appl. Phys.* **88**, 1073–1081 (2000).
18. Kobrak, M. N. & Bittner, E. R. Quantum molecular dynamics study of polaron recombination in conjugated polymers. *Phys. Rev. B* **62**, 11473–11486 (2000).
19. Blom, P. W., de Jong, M. J. M. & Breedijk, S. Temperature dependent electron-hole recombination in polymer light emitting diodes. *Appl. Phys. Lett.* **71**, 930–932 (1997).
20. Pope, M. & Swenberg, C. E. *Electronic Processes in Organic Crystals and Polymers* 2nd edn, 958–960 (Oxford Science, Oxford, 1999).
21. Shuai, Z., Beljonne, D., Silbey, R. J. & Brédas, J. L. Singlet and triplet exciton formation rates in conjugated polymer light-emitting diodes. *Phys. Rev. Lett.* **84**, 131–134 (2000).
22. Hong, T. & Meng, H. Spin-dependent recombination and electroluminescence quantum yield in conjugated polymers. *Phys. Rev. B* **63**, 1–5 (2001).
23. Burin, A. L. & Ratner, M. A. Spin effects on the luminescence yield of organic light emitting diodes. *J. Chem. Phys.* **109**, 6092–6102 (1998).

**Acknowledgements**

We thank N. C. Greenham for discussions and M. R. A. Al-Mandhary for the synthesis of the polymer and monomer. A.K. thanks Peterhouse, University of Cambridge, UK, for a Fellowship and the Royal Society for a University Research Fellowship. M.S.K. thanks Sultan Qaboos University, Oman, for a research grant and research leave, and the EPSRC (UK) for a Visiting Fellowship. This work was funded by the EPSRC.

Correspondence and requests for materials should be addressed to A.K. (e-mail: ak10007@cam.ac.uk).

.....  
**Superconductivity in single crystals of the fullerene C<sub>70</sub>**

**J. H. Schön\*†, Ch. Kloc\*, T. Siegrist\*‡, M. Steigerwald‡, C. Svensson§ & B. Batlogg\*||**

\* Bell Laboratories, Lucent Technologies, 600 Mountain Avenue, Murray Hill, New Jersey 07974, USA  
 † Department of Physics, University of Konstanz, D-78457 Konstanz, Germany  
 ‡ Agere Systems, 600 Mountain Avenue, Murray Hill, New Jersey 07974, USA  
 § Inorganic Chemistry 2, PO Box 124, Lund University, S-221 00 Lund, Sweden  
 || Solid State Physics Laboratory ETH, CH-8093 Zürich, Switzerland

.....  
**The observation of superconductivity in doped C<sub>60</sub> has attracted much attention<sup>1–3</sup>, as these materials represent an entirely new class of superconductors. A maximum transition temperature (T<sub>c</sub>) of 40 K has been reported<sup>4</sup> for electron-doped C<sub>60</sub> crystals, while a T<sub>c</sub> of 52 K has been seen<sup>5</sup> in hole-doped crystals; only the copper oxide superconductors have higher transition temperatures. The results for C<sub>60</sub> raise the intriguing questions of whether conventional electron–phonon coupling alone<sup>1</sup> can produce such high transition temperatures, and whether even higher transition temperatures might be observed in other fullerenes<sup>6–8</sup>. There have, however, been no confirmed reports of superconductivity**

**in other fullerenes, though it has recently been observed in carbon nanotubes<sup>9</sup>. Here we report the observation of superconductivity in single crystals of electric-field-doped C<sub>70</sub>. The maximum transition temperature of about 7 K is achieved when the sample is doped to approximately four electrons per C<sub>70</sub> molecule, which corresponds to a half-filled conduction band. We anticipate superconductivity in smaller fullerenes at temperatures even higher than in C<sub>60</sub> if the right charge density can be induced.**

Metallic behaviour is expected for KC<sub>70</sub> and K<sub>4</sub>C<sub>70</sub> owing to the half-filling of the lowest unoccupied molecular orbital bands in K-intercalated C<sub>70</sub>. An initial transport study on K-intercalated C<sub>70</sub> found a maximum conductivity of ~2 S cm<sup>-1</sup> (ref. 10). Theory and experiment showed that K<sub>4</sub>C<sub>70</sub> exhibits a larger conductivity because of its higher density of states<sup>11–13</sup>. Pure C<sub>70</sub> and alkali-metal-doped C<sub>70</sub> show non-zero resistance down to 1.8 K. The absence of superconductivity in these experiments is not well understood, and might be related to disorder and structural defects in the K<sub>4</sub>C<sub>70</sub> thin films. A weak electron–phonon interaction<sup>11,14</sup> and a reduced density of states at the Fermi level<sup>15</sup> have also been invoked as reasons for the apparent lack of superconductivity. We note, however, that most experiments have been performed on polycrystalline material, and phase-pure alkali-doped C<sub>70</sub> analogues of A<sub>3</sub>C<sub>60</sub> have not been reported. In addition, various crystallographic structures of C<sub>70</sub> have been observed<sup>16</sup>. Here we have chosen a different approach to induce electric charge in C<sub>70</sub> crystals. We have recently demonstrated that the electrical properties of organic materials can be investigated over a wide range of charge density using field-effect doping, without inducing additional disorder<sup>5,17–19</sup>, leading to gate-induced superconductivity in a variety of molecular organic crystals<sup>5,17,18</sup>. This method therefore seems to be well suited to our investigation of the reasons for the absence of superconductivity in the higher fullerenes—is it related to intrinsic properties, or to difficulties in chemical doping? Here we apply this technique to investigate the possibility of superconductivity in high-quality C<sub>70</sub> single crystals.

We grew single crystals of C<sub>70</sub> (smaller than 1 mm<sup>3</sup>) from the vapour phase in a stream of hydrogen; the experimental conditions were similar to those used to grow C<sub>60</sub> (ref. 5). The crystals were annealed in a xenon atmosphere, but we detected no incorporation of the inert gas into the crystals. We performed an X-ray structural analysis of the C<sub>70</sub> single crystals, which showed them to be hexagonal closed packed (h.c.p.) C<sub>70</sub>, with lattice parameters *a* = 10.602(9) Å and *c* = 17.263(13) Å. Previous studies of hexagonal C<sub>70</sub> gave lattice parameters of *a* = 10.104 Å and *c* = 18.584 Å, with a wide mosaic spread of the order of a few degrees<sup>20</sup>—furthermore, these crystals showed diffuse rods typical of stacking faults<sup>21</sup>. In contrast, our crystals show a much narrower mosaic of the order of 0.4°. In addition, the *c/a* ratio for our crystals is close to the ideal value of 1.63 for sphere packing, in contrast to the reported value of 1.84. To first order, it is possible to approximate the ellipsoidal C<sub>70</sub> molecule by a hollow sphere with radius *r* = 3.78 Å, and we obtained a residual of *R* = 0.065 for 118 independent reflections measured. As stacking faults were expected to be present, we looked for diffuse rods of intensity. Instead, we found well developed superstructure reflections with a mosaic spread of the order of 0.4° consistent with 6H polytypes, leading to a tripling of the *c* axis (*3c* = 51.79 Å). Different 6H stacking sequences are expected, producing twinning at room temperature. On average, five layers are stacked coherently, with the sixth in either the h.c.p. or the cubic close packed (c.c.p.) position. Low-temperature X-ray diffraction revealed a further lowering of symmetry, but the crystals clearly undergo multiple twinning upon cooling. This lowering of the symmetry is indicative of a transition to a phase in which the C<sub>70</sub> molecules no longer rotate freely. However, we do not expect that the orientational order of the molecules will be complete, similar to the phase transition observed for C<sub>60</sub> upon cooling<sup>22</sup>. Further structural studies at low temperature are under way.